Asian Journal of Chemistry; Vol. 38, No. 3 (2026), 601-609
ASIAN JOURNAL OF CHEMISTRY
https://doi.org/10.14233/ajchem.2026.34781

Structural and Functional Optimisation of Lomustine through Hydroxypropyl-β-Cyclodextrin Complexation: *In vitro* and Computational Insights

SHANMUGAPRIYA ARUMUGAM[1], RUPA DEVI[2], BALAJI GANESH[2] and SIVAKAMAVALLI JEYACHANDRAN[3,*]

[1]Department of Chemistry, AAA College of Engineering and Technology, Amathur, Sivakasi-626005, India
[2]Department of Periodontics, Saveetha Dental College and Hospitals, Saveetha University, Chennai-600077, India
[3]Lab in Biotechnology and Biosignal Transduction, Department of Orthodontics, Saveetha Dental College and Hospital, Saveetha University, Chennai-600077, India

*Corresponding author: E-mail: sivakamavalli.sdc@saveetha.com

Received: 28 August 2025 *Accepted*: 19 December 2025 *Published online*: 6 March 2026 AJC-22278

This study reports the hydroxypropyl-β-cyclodextrin (HPβCD) complexation as an effective strategy to enhance the solubility and therapeutic efficacy of lomustine (LMT), a poorly water-soluble anticancer drug. Inclusion complexes were synthesized using physical mixing (PM) and microwave irradiation (MWI) methods and characterised with UV-Vis, FTIR, XRD, DSC and SEM techniques. Molecular docking studies confirmed the complex formation, revealing favourable binding energies of 4.1 and -6.4 kcal mol^{-1}. The LMT-HPBCD complex demonstrated significantly improved dissolution properties compared to pure LMT, with the microwave-irradiated complex showing particularly enhanced performance. *In vitro* cytotoxicity studies against U87-MG glioblastoma cells revealed superior anticancer activity for the complexed formulations, with cell viability reduced to 22.3-38.6% (*vs.* 45.7-69.8% for PM and 67.3-91.8% for pure LMT). These findings demonstrate that HPβCD complexation effectively enhances both the physico-chemical properties and biological activity of LMT, offering promising potential for improved glioblastoma treatment.

Keywords: Lomustine, Hydroxypropyl-β-cyclodextrin, Dissolution, Anticancer activity.

INTRODUCTION

Annually, around 21% of global deaths attributable to disease result from cancer, making it the second leading cause of mortality [1,2]. It is important to mention that brain cancer is particularly significant, in India. The International Agency for Research on cancer observed that about 28,000 cases of brain tumours are diagnosed and around 24,000 individuals die each year as a result [3,4]. Conventional cancer treatments, primarily chemotherapy, often cause severe side effects due to the non-selective action of drugs on both cancerous and healthy tissues. However, continuous research efforts over the years have led to the development of numerous anticancer drugs, derived from both synthetic and natural sources, aimed at improving treatment outcomes. Since 1970s, medical oncologists have relied on lomustine (LMT; 1-(2-chloroethyl)-3-cyclohexyl-1-nitrosourea), an alkylating anti-neoplastic medication, in cancer treatment. It is an especially strong nitrosourea, a group of anticancer agents that influence several types of leukemias and solid tumors.

Since LMT does not dissolve well in water [5-7], the degree of dissolution has a direct impact on the accuracy of the response obtained. Boosting oral drug solubility is a major obstacle for pharmaceutical companies [8,9]. There are several approaches used to increase the solubility of new chemical entities (NCEs), examples being physical and chemical modifications, making particles smaller, designing perfect crystals, adjusting pH, using co-solvents, hydrotropes, salts, solid dispersions, including surfactants and inclusion complexation [10,11].

Cyclodextrins (CDs) and their derivatives improve the solubility limited water solubility pharmaceuticals through the formation of inclusion complexes [12-14]. CDs are cyclic oligosaccharides formed from α-1,4-linked glucose units, resulting in a distinctive molecular structure characterized by a hydrophilic exterior and a comparatively hydrophobic inner cavity. This configuration allows for the encapsulation of lipophilic medicinal molecules within the cavity while maintaining compatibility with aquatic conditions. Despite the water solubility of these native CDs and their complexes, their aqueous

solubility is constrained, especially for βCD. To mitigate this constraint, additional water-soluble βCD derivatives, *e.g.*, hydroxypropyl-β-cyclodextrin (HPβCD) and sulfobutylether-β-cyclodextrin sodium (SBEβCD), are frequently utilized in the formulation of injectable and intravenous pharmaceutical products [15-17].

Previous research has reported the interaction of LMT with β-cyclodextrin in terms of spectrofluorimetric analysis, thermal stability and degradation behaviour [18,19]. In contrast, the current work involves to improve the solubility, dissolving rate and anticancer activity of LMT. Molecular docking was used to investigate the interaction between LMT and hydroxypropyl-β-cyclodextrin (HPβCD), and also investigate the different synthetic methods affect solubility. Two different techniques, namely mechanical trituration and microwave irradiation for the synthesis of inclusion complex. The complex was characterised with Fourier transform infrared spectroscopy (FT-IR), powder X-ray diffraction (PXRD), differential scanning calorimetry (DSC) and scanning electron microscopy (SEM). The cytotoxic activity of LMT was evaluated and compared before and after complexation to assess the impact of inclusion on its biological performance. Furthermore, the molecular docking studies were conducted to support and validate the binding interactions between LMT and HPβCD suggested by the solid-state characterisation results.

EXPERIMENTAL

Lomustine (LMT) and 2-hydroxypropyl-β-cyclodextrin (HPβCD, average substitution degree = 1380) were supplied by Aldrich Chemical Inc. and ABCR GmbH and Co. KG, respectively and used as received. Other reagents and chemicals used were of analytical reagent quality. All the experiments were performed using ultrapure water. The U-87 MG cell line, derived from a glioblastoma-astrocytoma in humans, was obtained from ATCC (HTB-14) and Eagle's minimum essential medium was obtained from ATCC (#400-NL-1). The HBMECs and the full HBMEC medium from Cell Systems Corporation were used, supplemented with recombinant growth factors from CultureBoost-R.

Synthesis of inclusion complex

Physical mixing (PM): Lomustine (LMT) and hydroxypropyl-β-cyclodextrin (HPβCD) (Fig. 1) were weighed in a 1:1 molar ratio and homogenised by vigorous trituration in a mortar for 3 h, then passed through No. 44 sieve and stored in airtight containers until further use [20,21].

Microwave irradiation method: The LMT and HPβCD components were precisely weighed in 1:1 molar ratio, mixed and then aqueous ethanol was gradually added while blending the components until a homogeneous paste was formed. The sample was transferred into a separate beaker and irradiated individually in a microwave set to 500 W (Samsung model ME0113M1, South Korea) following the reported method [22,23]. The irradiated samples were agitated to achieve a homogeneous inclusion complex (Fig. 2). The product was then cooled, collected and stored in a desiccator for 2 days to remove any remaining moisture.

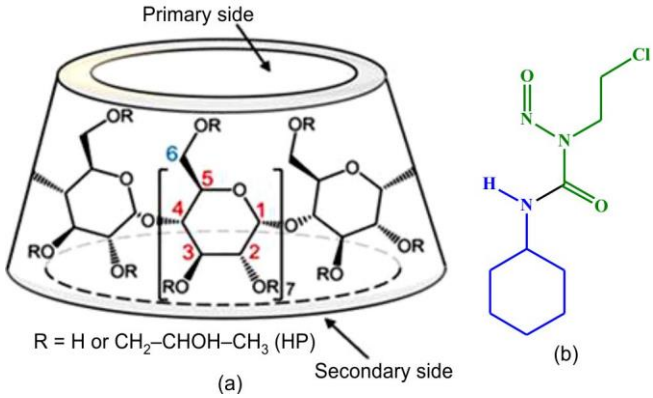

Fig. 1. Chemical structure of (a) HPβCD and (b) drug lomustine

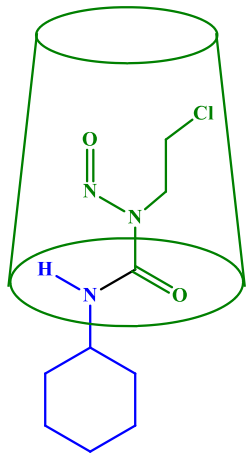

Fig. 2. Schematic representation of inclusion complex of LMT:HPβCD

Phase solubility studies: The solubilizing capacity of HPβCD toward LMT was evaluated using the phase-solubility method, which also enabled determination of the stability constant of the resulting complex [24,25]. In accordance with the procedure described by Higuchi & Connors [24], an excess amount of LMT (100 mg) was added to 50 mL of distilled water containing varying concentrations of HPβCD to establish the solubility profile. All mixtures were agitated in a thermostatic bath at 37 ± 1 ºC for 48 h to achieve equilibrium. Aliquots were taken using a syringe, passed through a 0.45 µm PVDF membrane and then diluted. Sample was investigated with the Shimadzu UV-1700 UV spectrophotometer at 232 nm. Experiments to assess solubility were done three times independently. Phase-solubility diagrams (PSDs) were constructed to evaluate the complexation behaviour between the drug and HPβCD and to determine the apparent stability constant (K_c) for a presumed 1:1 inclusion complex using the appropriate mathematical relationship. The nature of the drug-HPβCD interaction was interpreted from the solubility profile, and the K_c value was subsequently calculated according to the Higuchi & Connors equation [24]:

$$K_s = \frac{\text{Slope}}{S_o(1-\text{Slope})}$$

where slope was obtained from the linear portion of phase solubility diagram and S_o is the intrinsic solubility of drug.

***In vitro* dissolution studies:** To carry out the dissolution investigation, samples of LMT and the inclusion complexes

were deposited in a dissolution device with of phosphate buffer saline (PBS, 900 mL) media at a pH of 6.4 and 37 ± 0.5 ºC. At the predetermined intervals, 5 mL aliquots were withdrawn and immediately replaced with equal volume of fresh release medium. The collected samples then diluted, filtered and analysed at 232 nm for drug content using a UV-visible spectrophotometer [21,25-27].

Dissolution testing was conducted in a paddle-style apparatus running at 50 revolutions per min. Samples were obtained at time intervals of 5, 10, 15, 30, 45 and 60 min. The solutions were filtered and examined to establish the patterns of SV-409 formulation release. Appropriate positive and negative controls were used to confirm the accuracy of the cytotoxicity test.

Anticancer activity: The U87-MG cell line, derived from human glioblastoma-astrocytoma, along with EMEM, was obtained from ATCC. In brief, U87-MG cells were cultured in EMEM supplemented with 10% fetal bovine serum (FBS) and 1% antibiotic-antimycotic solution. The DB029 and MHBT161 cell lines were maintained in DMEM with similar supplementation of 10% FBS and 1% antibiotic-antimycotic solution. Human brain microvascular endothelial cells (HBMECs), a primary cell line, were grown in CSC complete medium enriched with 10% FBS and CultureBoost-R recombinant growth factors, following the manufacturer's protocol. All cell lines were incubated at 37 ºC in a humidified atmosphere containing 5% CO_2. The viability of cells was measured and the IC_{50} values were calculated to evaluate the concentration inhibiting 50% growth.

***In vitro* cell viability assay:** Cell viability tests using the MTT method were done on both LMT and the LMT-HPβCD complex. The cells were dissociated with trypsin, collected under aseptic circumstances, identified and adjusted to a density of 5×10^3 cells per well. Each well of a 96-well plate received 100 µL of sterile culture media, followed by the seeding of cells as previously outlined [28-30]. Following a 24 h incubation period, the cells were administered different dosages (50-450 µM) of either the free drug or its inclusion complex and incubated for an additional 48 h. Subsequent to treatment, 50 µL of MTT solution was introduced to each well and the plates were incubated in dark for 3 h to facilitate formazan crystal formation. The medium was subsequently extracted and the resultant crystals were dissolved in 50 µL of isopropanol. The plates were agitated for a minimum of 3 min to ensure the complete dissolution and finally the absorbance was recorded at 600 nm using a microplate reader after 5 min. For, control experiments, Ham's F-12 medium (pH 7.4) and Dulbecco's phosphate-buffered saline (PBS) were used.

Molecular docking: Docked HPβCD:LMT models were evaluated based on the interface area, shape, interactions from van der Waals, hydrogen bonding and other interaction energies. The top model, with the highest shape compatibility (3370), largest interface area (646 $Å^2$) and the lowest atomic contact energy (288.26 kJ mol^{-1}), represented the most favourable complex (Fig. 3) [31]. AutoDock analysis confirmed the optimal global energy and balanced attractive and repulsive van der Waals interactions, with the LMT molecule fitting comfortably into HPβCD's hydrophobic cavity, likely displacing water molecules through van der Waals forces, making it the preferred computational model.

RESULTS AND DISCUSSION

Phase solubility studies: The interaction between the ligand (HPβCD) and LMT was evaluated and the results are summarized in Table-1. A phase-solubility plot showed a linear relationship with a slope of 0.2389, indicating that drug solubility increases proportionally with the concentration of HPβCD (Fig. 4). According to the classification of Higuchi & Connors [24], this profile corresponds to an AL-type curve with a 1:1 stoichiometry [25], suggesting the suitability of preparing a water-compatible drug-HPβCD inclusion complex. The apparent host-guest stability constant (K_c) was calculated as 843.68 M^{-1} [32], reflecting a strong interaction between the poorly water-soluble drug LMT and HPβCD, which supports the formation of a stable inclusion complex.

FT-IR studies: The FTIR spectra (Fig. 5) show the functional groups present in HPβCD, LMT and their resultant solid inclusion complexes (LMT-HPβCD). When HPβCD

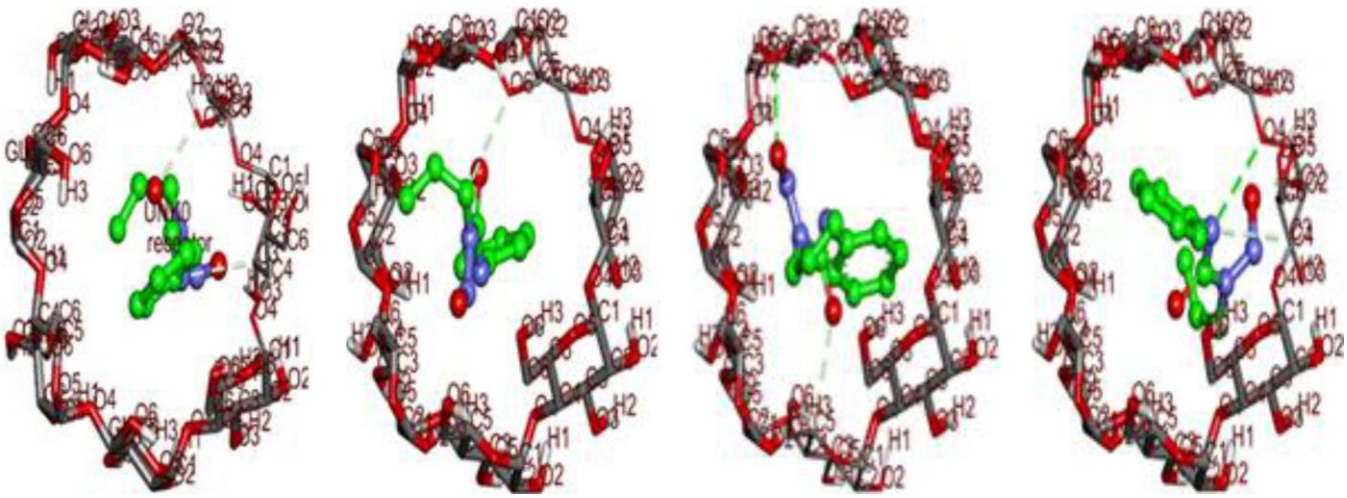

Fig. 3. Molecular docking interaction of LMT with HPβCD cavity in inclusion

TABLE-1
ABSORPTION MAXIMA AND ABSORBANCE
VALUES OF PHASE SOLUBILITY STUDIES

Concentration of HP-β-CD (mmol)	λ_{max} (nm)	Absorbance
0	232	0.6824
0.002	232	0.8326
0.004	232	1.0214
0.006	232	1.4836
0.008	232	1.6326
0.010	232	1.7311
0.012	232	1.9112

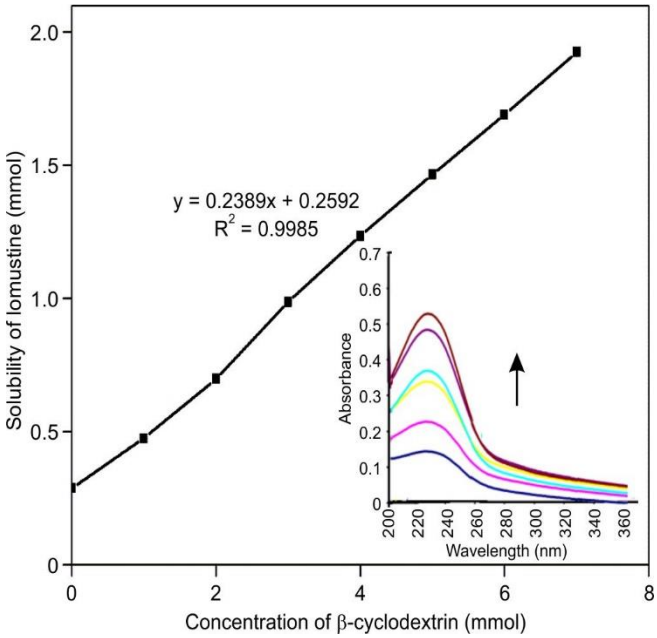

Fig. 4. Phase solubility profile of drug LMT-HPβCD

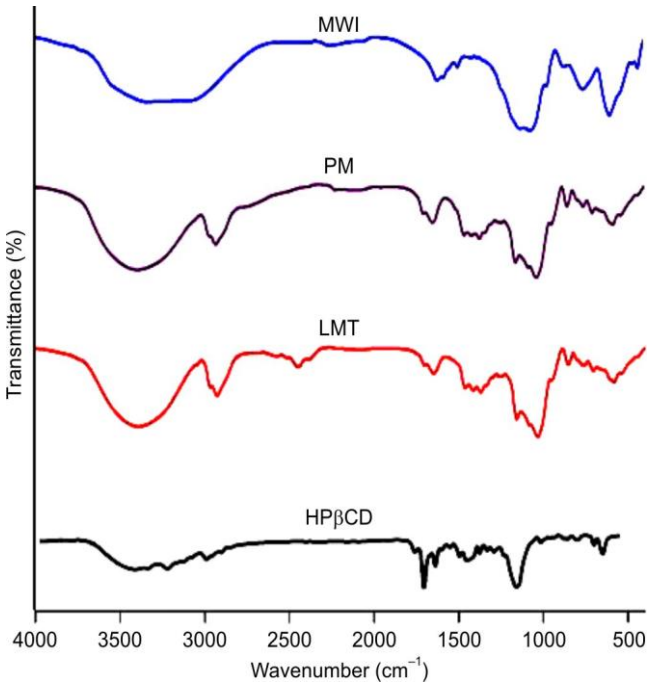

Fig. 5. FT-IR spectra of HPβCD, LMT, LMT-HPβCD (PM) and LMT-HPβCD (MWI)

forms a complex with another molecule, the characteristic bands in its spectrum may show subtle changes. These can include shifts in wavelength or variations in the intensity of the bands. These modifications are typically due to the interaction with the part of the guest molecule, which is encapsulated within the HPβCD cavity. The FT-IR spectrum of HPβCD displays a prominent absorption band at 3431 cm^{-1}, attributed to the O–H stretching vibration. Furthermore, a peak observed in the 3000-2800 cm^{-1} range corresponds to the stretching vibrations of C-H and CH_2 groups. The bands at 1028 cm^{-1} and 1156 cm^{-1} are associated with the stretching vibrations of the C–OH and C–O–C groups in the HPβCD molecule [33,34].

In LMT, the absorption peak observed at 3350 cm^{-1} corresponds to the N–H stretching vibration. The peaks at 2939 cm^{-1} and 2857 cm^{-1} are attributed to C–H stretching vibrations characteristic of alkanes, while the peak at 1440 cm^{-1} corresponds to the C–H bending vibrations. The strong absorption at 1707 cm^{-1} is assigned to the carbonyl (C=O) stretching vibration, whereas the peak at 1536 cm^{-1} is due to the N=O stretching vibration. The absorption peaks at 1486 and 720 cm^{-1} are attributed to the presence of multiple $–CH_2$ groups [35].

In LMT-HPβCD (PM), the spectrum represents the physical mixture of HPβCD and LMT, the distinctive absorption peaks of LMT at 3350 cm^{-1}, 2939 cm^{-1}, 2857 cm^{-1}, 1536 cm^{-1} and 1486 cm^{-1} are all present, alongside the peaks at 3393 cm^{-1} and 1032 cm^{-1}. This suggests that the physical mixture is the superimposition of host and guest does not result in the inclusion complex formation [36]. The major change seen in LMT-HPβCD (MWI), is the significant reduction in the O–H stretch at 3393 cm^{-1} and the disappearance of N–H and C=O stretching vibrations at 3350 cm^{-1} and 1707 cm^{-1}, as well as N–H, C=O and C–H in LMT at 2857 cm^{-1} and 2939 cm^{-1}. This indicates that HPβCD and LMT can successfully form an inclusion complex, as evidenced by the alterations in the microenvironment of both the host and the guest upon complexation [37].

XRD studies: The X-ray diffraction pattern of LMT exhibited sharp and intense peaks at 8.2º, 18.4º, 22.4º and 23.2º (2θ), which are the characteristic of its crystalline nature [38]. HPβCD was identified as amorphous since no any crystalline peaks were observed [39] (Fig. 6). The XRD patterns of the physical mixture primarily reflected the amorphous nature of HPβCD, with only a few characteristic peaks corresponding to crystalline LMT. In contrast, the MWI-inclusion complex displayed a fully amorphous diffraction pattern, likely due to the combined effects of microwave treatment and the inherent amorphous structure of HPβCD, indicating the absence of crystalline LMT. These findings are consistent with the FT-IR results, confirming that LMT was successfully incorporated into HPβCD as an inclusion complex.

SEM studies: Although the SEM images indicate the potential inclusion complex formation, they may not be solely sufficient for definitive confirmation. The SEM images of pure LMT (Fig. 7a) displayed larger particles with a rough surface texture. In contrast, HPβCD appeared as irregular aggregates of varying sizes without a distinct structure which

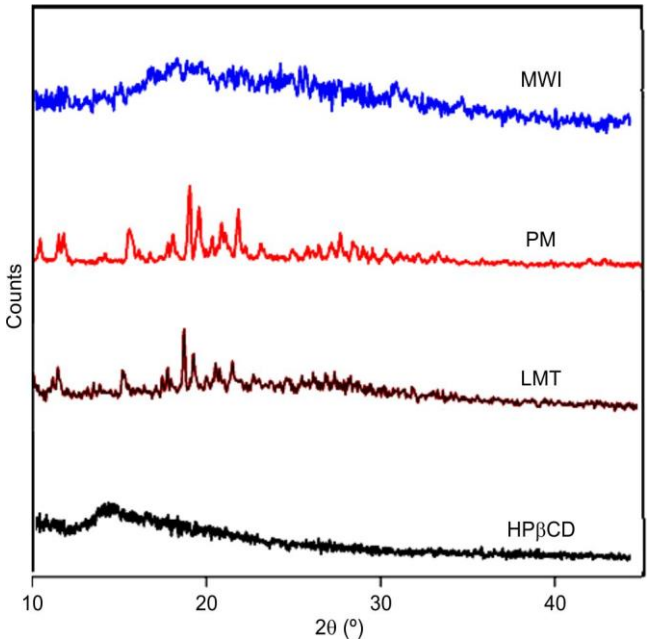

Fig. 6. XRD spectra of HPβCD, LMT, LMT-HPβCD (PM) and LMT-HPβCD (MWI)

is shown in Fig. 7b. The physical mixture of LMT and HPβCD did not show a homogeneous or spherical particle shape (Fig. 7c). In comparison, the inclusion complex prepared using the MWI method exhibited a markedly different morphology (Fig. 7d). The SEM images revealed needle-like crystals that aggregated into structures resembling shrinked cylindrical spheres. This variation in morphological arrangement supports the conclusion that inclusion complexes may have formed [39].

***In vitro* dissolution studies:** The dissolution rates of all LMT-HPβCD complexes were consistently higher than that of pure LMT across all recorded time points. Significantly, inclusion complexes prepared with HPβCD (MWI) dissolved significantly faster than simple physical mixture of HPβCD and LMT (Figs. 8 and 9) [40,41]. Increasing the HPβCD content further enhanced the dissolution rate of the inclusion complexes (Table-2). The improved dissolution can be attributed to the water-soluble nature of the HPβCD inclusion complexe. As HPβCD consist of a hydrophobic cavity that naturally traps high-energy water molecules displaced when hydrophobic LMT molecules are incorporated. This encapsulation process occurs through weak, non-covalent interactions

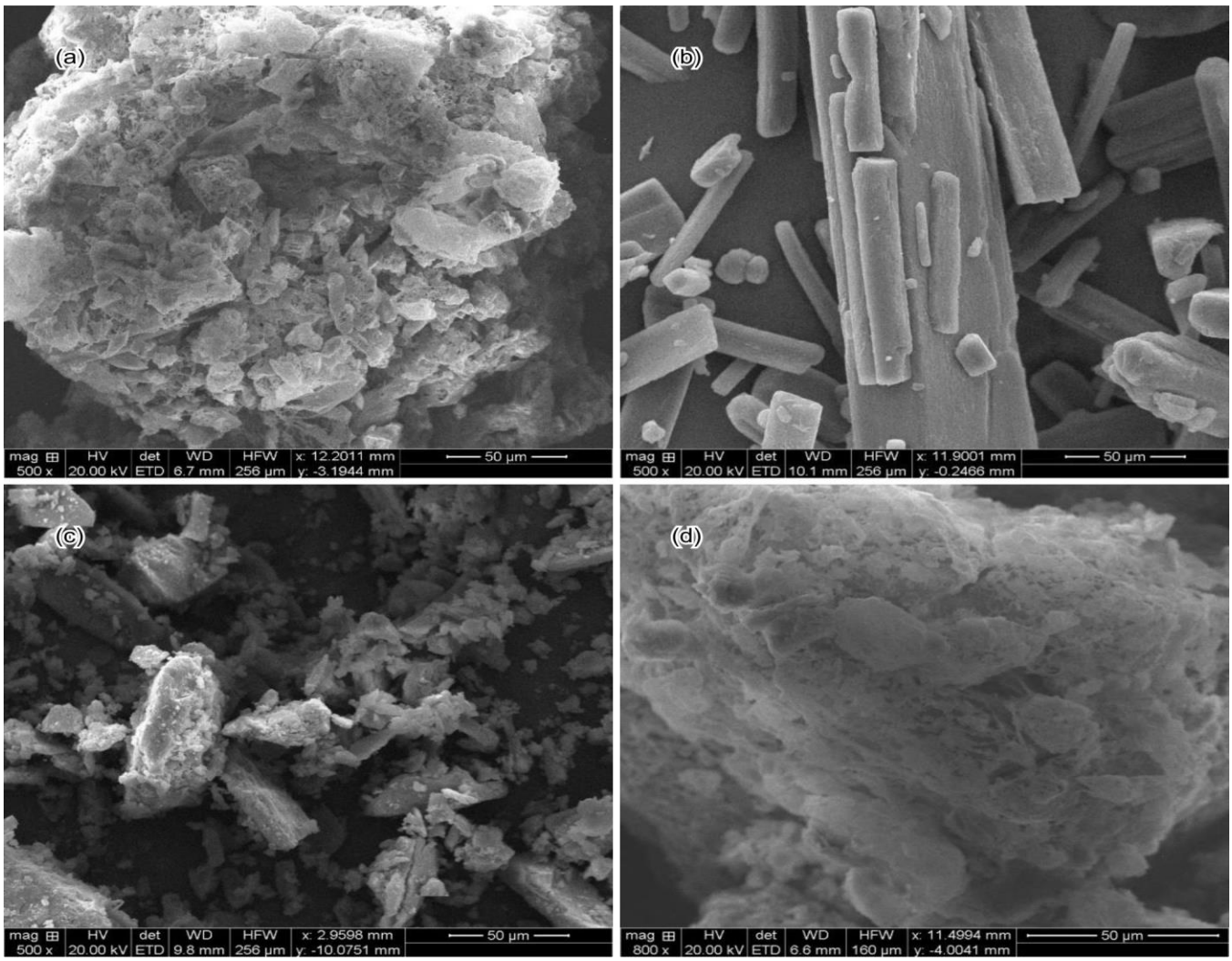

Fig. 7. SEM images of (a) HPβCD, (b) LMT, (c) LMT-HPβCD (PM) and (d) LMT-HPβCD (MWI)

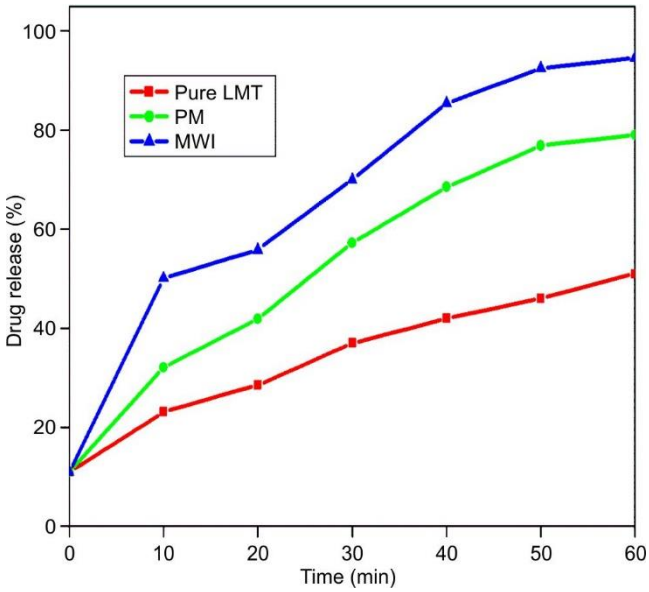

Fig. 8. Dissolution drug release profiles for HPβCD, LMT, LMT-HPβCD (PM) and LMT-HPβCD (MWI)

TABLE-2
PERCENTAGE OF *in vitro* DRUG RELEASE PROFILE OF LMT-β-CD INCLUSION COMPLEXES IN pH ~7.4 MEDIUM AT 37 ºC

Methods of preparation	Drug released (%)
Pure LMT	36
Physical mixture	58
Microwave irradiation method	83

between the hydrophobic regions of HPβCD and the drug, effectively trapping the guest molecule within the cyclodextrin structure. As a result, the hydrophobic LMT is shielded from the aqueous environment, enhancing its apparent solubility and dissolution rate [42,43]. Moreover, the surfactant-like properties of HPβCD contribute to faster drug release. By reducing the interfacial tension between the hydrophobic drug particles and the surrounding aqueous medium, HPβCD promotes better wetting and dispersion of LMT, further facilitating rapid dissolution [44,45]. Even in physical mixtures, the presence of water-soluble HPβCD improves the interaction between the drug's hydrophobic surface and water,

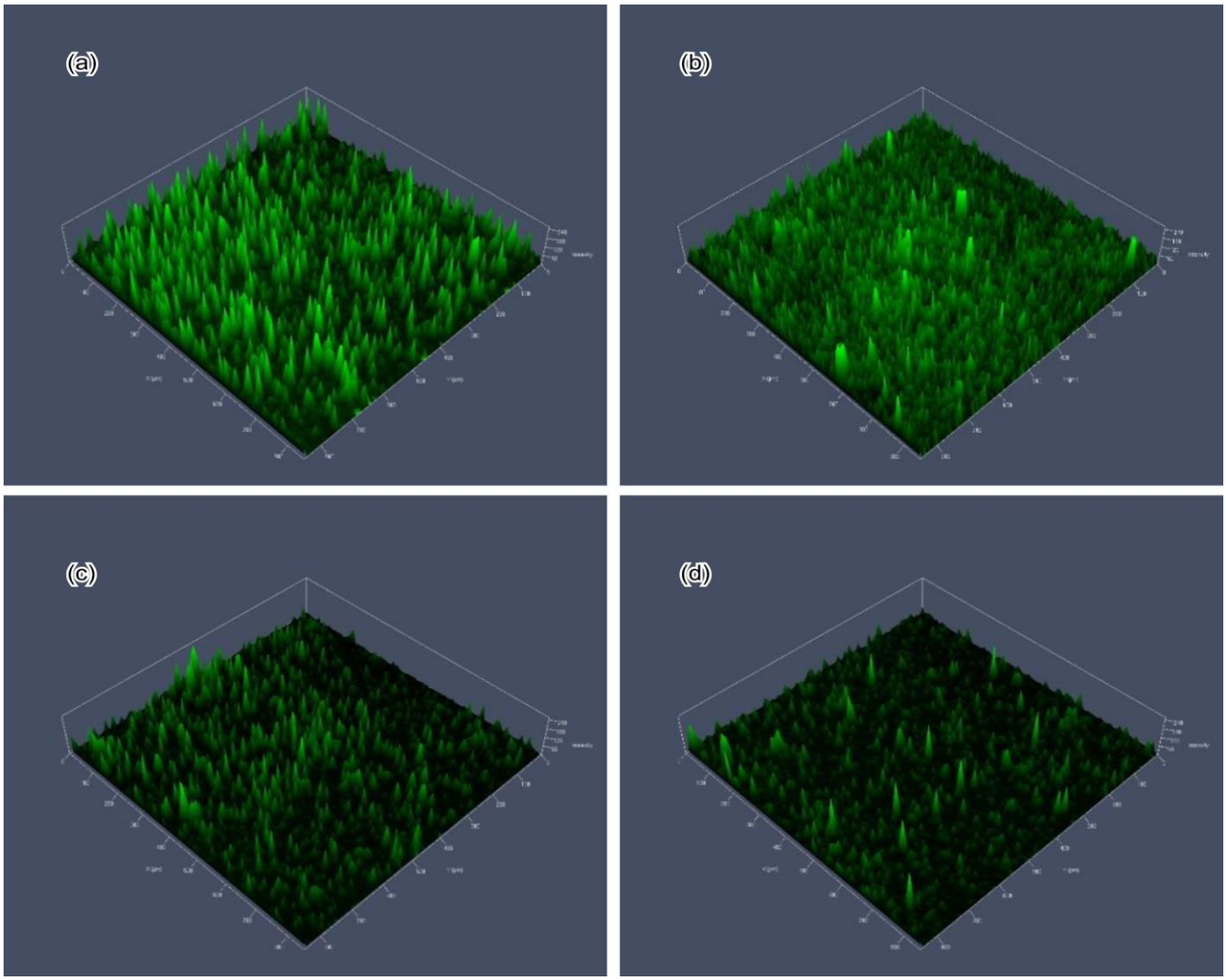

Fig. 9. Microscopic images showing the inhibition of the biofilm formed by human brain (U87-MG cell line) cancer cells in the presence of the (a) control, (b) LMT, (c) LMT-HPβCD (PM) and (d) MT-HPβCD (MWI)

marginally increasing solubility, although not as effectively as in true inclusion complexes.

***In vitro* cytotoxicity:** The *in vitro* cytotoxicity of HPβCD: LMT inclusion complexes on U87-MG cells was assessed using the MTT assay. The results indicated a dose-dependent decrease in cell viability following treatment with various concentrations (20-100 μg/mL) (Fig. 10). The percentage cell viability obtained for the individual complex ranged between 22.3-38.6%, 45.7-69.8%, 67.3-91.8% for the cells treated with LMT, LMT-HPβCD (PM), LMT-HPβCD (MWI) methods, respectively [46]. The *in vitro* cytotoxicity of LMT-HPβCD was evaluated in U87-MG cells, demonstrating an enhanced cytotoxic effect compared to complexes prepared by physical mixture (PM) and microwave irradiation (MWI), as well as pure LMT at equivalent doses.

As a result, it is clear that HPβCD:LMT inclusion complexes demonstrated safety and non-toxicity, making them promising candidates for further anticancer evaluation. Confocal laser scanning microscopy (CLSM) revealed that HPβCD facilitates cellular uptake of LMT, localizing near the nucleus and modifying U87-MG cell morphology within 24 h. Cells treated with the complexes displayed stretched, elliptical nuclei, indicating significant cytotoxic effects compared to LMT alone or the physical mixture with HPβCD. Microwave-irradiated complexes showed superior performance in anticancer activity, suggesting that HPβCD binds LMT more efficiently than βCD, with hydroxypropyl substitution groups enhancing both drug encapsulation and cellular delivery [47,48].

The hydrophobic cavity of HPβCD allows LMT to be sequestered from the aqueous environment and integrated into cell membranes, improving absorption and interaction with intracellular targets. At a concentration of 100 μg/mL, the HPβCD:LMT complex completely inhibited cancer cell activity, demonstrating enhanced cellular uptake and efficacy compared to βCD-based complexes. These observations indicate that complexation with HPβCD not only improves solubility and thermal stability but also significantly boosts the anticancer potential of LMT in vitro. These findings suggest

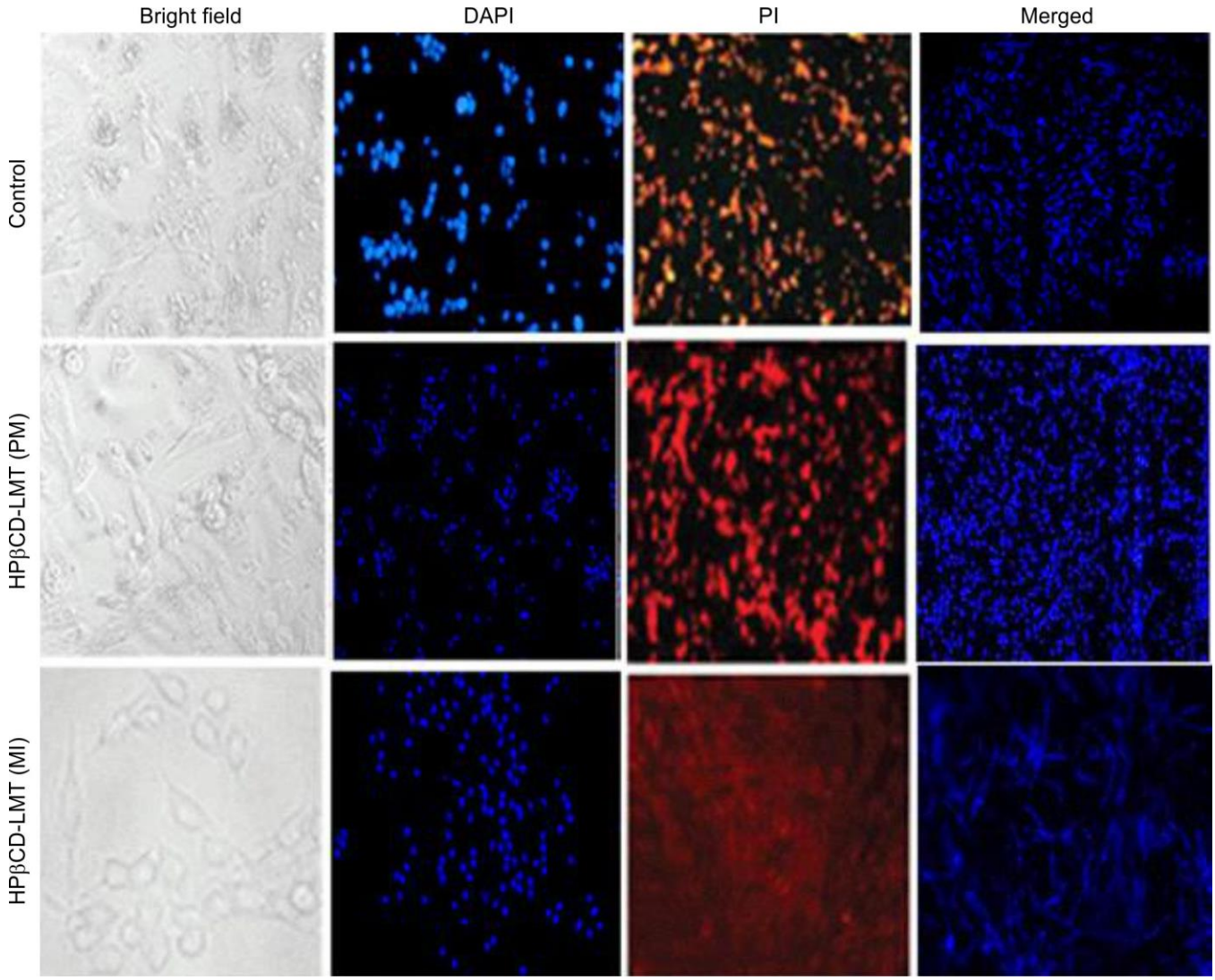

Fig. 10. Confocal microscopic images of the microwave irradiated inclusion complex-treated human brain (U87-MG cell line) cancer cells were stained with DAPI and PI aftertreatment with the inclusion complexes LMT- HPβCD (100 μg/mL) for 24 h. Cells treated with free LMT-HPβCD (100 μg/mL) were used as a control. Scale bar = 100 nm.

that HPβCD could serve as an effective carrier for LMT in the therapeutic applications, although *in vivo* studies are essential to validate clinical efficacy and safety, particularly at higher doses.

Conclusion

The study successfully developed lomustine (LMT)-HPβCD inclusion complexes using physical mixing (PM) and microwave irradiation (MWI) methods. Comprehensive characterisation *via* FTIR, XRD and SEM confirmed the successful complex formation, while the phase solubility studies revealed a 1:1 stoichiometry with a stability constant (K_c) of 843.68 M^{-1}. Molecular docking further validated the interactions, with favourable binding scores supporting the experimental results. The LMT-HPβCD complexes exhibited significantly enhanced dissolution rates compared to pure LMT, with the microwave-irradiated formulation showing the most pronounced improvement. Significantly, the CD inclusion complexes demonstrated superior cytotoxic effects against U87-MG glioblastoma cells, highlighting their potential for improved therapeutic efficacy. Among the preparation methods, MWI yielded the most promising results, suggesting its advantage for the scalable production. Investigating the formulation optimisation and scale-up protocols could promote the successful application of LMT-HPβCD pharmacokinetic enhancements in the development of new drug formulations.

CONFLICT OF INTEREST

The authors declare that there is no conflict of interests regarding the publication of this article.

DECLARATION OF AI-ASSISTED TECHNOLOGIES

During the preparation of this manuscript, the authors used an AI-assisted tool(s) to improve the language. The authors reviewed and edited the content and take full responsibility for the published work.

REFERENCES

1. D.S. Shewach and R.D. Kuchta, *Chem. Rev.*, **109**, 2859 (2009); https://doi.org/10.1021/cr900208x
2. H.S. Hwang, H. Shin, J. Han and K. Na, *J. Pharm. Investig.*, **48**, 143 (2018); https://doi.org/10.1007/s40005-017-0377-x
3. R. Quan, H. Zhang, Z. Li and X. Li, *Medicine*, **99**, e18591 (2020); https://doi.org/10.1097/MD.0000000000018591
4. R. Stupp, W.P. Mason, M.J. van den Bent, M. Weller, B. Fisher, M.J.B. Taphoorn, K. Belanger, A.A. Brandes, C. Marosi, T. Gorlia, R.C. Janzer, U. Bogdahn, J. Curschmann, J.G. Cairncross, S.K. Ludwin, A. Allgeier, D. Lacombe, E. Eisenhauer and R.O. Mirimanoff, *N. Engl. J. Med.*, **352**, 987 (2005); https://doi.org/10.1056/NEJMoa043330
5. G. Gallant, R. Salvador and H. Dulude, *Bioorg. Med. Chem. Lett.*, **4**, 2353 (1994); https://doi.org/10.1016/0960-894X(94)85039-9
6. C.T. Gnewuch and G. Sosnovsky, *Chem. Rev.*, **97**, 829 (1997); https://doi.org/10.1021/cr941192h
7. C.R. Bethune, R.J. Geyer, A.M. Spence and R.J.Y. Ho, *Cancer Res.*, **61**, 3669 (2001).
8. B. Bittner and R.J. Mountfield, *Curr. Opin. Drug Discov. Devel.*, **5**, 59 (2002).
9. L.-Y. Lim and M.-L. Go, *Eur. J. Pharm. Sci.*, **10**, 17 (2000); https://doi.org/10.1016/S0928-0987(99)00084-6
10. E. Merisko-Liversidge, G.G. Liversidge and E.R. Cooper, *Eur. J. Pharm. Sci.*, **18**, 113 (2003); https://doi.org/10.1016/S0928-0987(02)00251-8
11. J.K. Spence, S.N. Bhattachar, J.A. Wesley, P.J. Martin and S.R. Babu, *Drug Dev. Ind. Pharm.*, **10**, 451 (2005).
12. O.E. Nicolaescu, I. Belu, A.G. Mocanu, V.C. Manda, G. Rău, A.S. Pîrvu, C. Ionescu, F. Ciulu-Costinescu, M. Popescu and M.V. Ciocîlteu, *Pharmaceutics*, **17**, 288 (2025); https://doi.org/10.3390/pharmaceutics17030288
13. C. Tsunoda, K. Hasegawa, R. Hiroshige, T. Kasai, H. Yokoyama and S. Goto, *Mol. Pharmaceutics*, **20**, 5032 (2023); https://doi.org/10.1021/acs.molpharmaceut.3c00291
14. I. Spiridon and N. Anghel, *Molecules*, **30**, 3044 (2025); https://doi.org/10.3390/molecules30143044
15. C.M. Fernandes, M. Teresa Vieira and F.J. B. Veiga, *Eur. J. Pharm. Sci.*, **15**, 79 (2002); https://doi.org/10.1016/S0928-0987(01)00208-1
16. S.W. Jun, M.S. Kim, J.S. Kim, H.J. Park, S. Lee, J.S. Woo and S.J. Hwang, *Eur. J. Pharm. Biopharm.*, **66**, 413 (2007); https://doi.org/10.1016/j.ejpb.2006.11.013
17. C.A. Ventura, I. Giannone, T. Musumeci, R. Pignatello, L. Ragni, C. Landolfi, C. Milanese, D. Paolino and G. Puglisi, *Eur. J. Med. Chem.*, **41**, 233 (2006); https://doi.org/10.1016/j.ejmech.2005.11.002
18. H. Fisli, N. Bensouilah, N. Dhaoui and M. Abdaoui, *J. Incl. Phenom. Macrocycl. Chem.*, **73**, 369 (2012); https://doi.org/10.1007/s10847-011-0073-9
19. I. Khan, J. Pandit, S. Ahmed, S. Zameer, S.A. Nikita, S. Ahmad, S. Bano, M.D. Ansari, P. Solanki, R.N. Jahan, A. Waheed, M. Aqil and Y. Sultana, *J. Drug Deliv. Sci. Technol.*, **75**, 103685 (2022); https://doi.org/10.1016/j.jddst.2022.103685
20. R.N. Marreto, E.E.C.V. Almeida, P.B. Alves, E.S. Niculau, R.S. Nunes, C.R.S. Matos and A.A.S. Araújo, *Thermochim. Acta*, **475**, 53 (2008); https://doi.org/10.1016/j.tca.2008.06.015
21. N. Ozdemir and S. Ordu, *Drug Dev. Ind. Pharm.*, **24**, 19 (1998); https://doi.org/10.3109/03639049809082348
22. M. Moneghini, B. Bellich, P. Baxa and F. Princivalle, *Int. J. Pharm.*, **361**, 125 (2008); https://doi.org/10.1016/j.ijpharm.2008.05.026
23. M. Cirri, F. Maestrelli, N. Mennini and P. Mura, *J. Pharm. Biomed. Anal.*, **50**, 683 (2009); https://doi.org/10.1016/j.jpba.2008.11.003
24. T. Higuchi and K.A. Connors, Advances in Analytical Chemistry and Instrumentation, Wiley, New York, vol. 4, pp. 117-212 (1965).
25. T. Loftsson, M. Masson and M.E. Brewster, *J. Pharm. Sci.*, **93**, 1091 (2004); https://doi.org/10.1002/jps.20047
26. P. Mura, M.T. Faucci and P.L. Parrini, *Drug Dev. Ind. Pharm.*, **27**, 119 (2001); https://doi.org/10.1081/DDC-100000478
27. S. Scalia, S. Villani, A. Scatturin, M.A. Vandelli and F. Forni, *J. Pharm. (Cairo)*, **175**, 205 (1998).
28. A.W. Bauer, W.M. Kirby, J.C. Sherris and M. Turck, *Am. J. Clin. Pathol.*, **45(4_ts)**, 493 (1966); https://doi.org/10.1093/ajcp/45.4_ts.493
29. T. Mosmann, *J. Immunol. Methods*, **65**, 55 (1983); https://doi.org/10.1016/0022-1759(83)90303-4
30. C. Zhang, G. Vasmatzis, J.L. Cornette and C. DeLisi, *J. Mol. Biol.*, **267**, 707 (1997); https://doi.org/10.1006/jmbi.1996.0859
31. P. Ahmadi and J.B. Ghasemi, *J. Incl. Phenom. Macrocycl. Chem.*, **79**, 401 (2013); https://doi.org/10.1007/s10847-013-0363-5
32. T. Brewster and T. Loftsson, *Adv. Drug Deliv. Rev.*, **597**, 66617 (2007); https://doi.org/10.1016/j.addr.2007.05.012
33. Y. Nakai, K. Yamamoto, K. Terada and H. Horibe, *J. Incl. Phenom.*, **2**, 523 (1984); https://doi.org/10.1007/BF00662218
34. R.O. Williams III, V. Mahaguna and M. Sriwongjanya, *Eur. J. Pharm. Biopharm.*, **46**, 355 (1998); https://doi.org/10.1016/S0939-6411(98)00033-2
35. S. Agarwal, D. Jangir, P. Singh and R. Mehrotra, *J. Photochem. Photobiol. B: Biology*, **130**, 281 (2014); https://doi.org/10.1016/j.jphotobiol.2013.11.017

36. V. Nikolic, S. Ilic-Stojanovic, L. Nikolic, M. Cakic, A. Zdravkovic, A. Kapor and M. Popsavin, *Hem. Ind.*, **68**, 107 (2014); https://doi.org/10.2298/HEMIND130306034N
37. P. Paul, U. Gupta, R. Kumar, S. Munagalasetty, H.P. Padhy, R. Nair, S. Mahajan, I. Maji, M. Aalhate, V. Bhandari, S.K. Guru and P.K. Singh, *J. Mol. Liq.*, **399**, 124458 (2024); https://doi.org/10.1016/j.molliq.2024.124458
38. C. Sonia, N. Chetry, T.G. Devi and T. Karlo, *Spectrosc. Lett.*, **57**, 128 (2024); https://doi.org/10.1080/00387010.2024.2330605
39. A. Ahad, Y.A. Bin Jardan, M.Z. Hassan, M. Raish, A. Ahmad, A.M. Al-Mohizea and F.I. Al-Jenoobi, *Drug Deliv.*, **29**, 1512 (2022); https://doi.org/10.1080/10717544.2022.2072540
40. B. Khatun, P. Baishya, A. Ramteke and T.K. Maji, *New J. Chem.*, **44**, 4887 (2022); https://doi.org/10.1039/C9NJ04408F
41. B. Guo, S. Zhong, N. Li, X. Li, J. Yi and M. Jin, *Drug Dev. Ind. Pharm.*, **39**, 1638 (2013); https://doi.org/10.3109/03639045.2012.728231
42. A.P. Mukne and M.S. Nagarsenker, *AAPS PharmSciTech*, **5**, 142 (2004); https://doi.org/10.1208/pt050119
43. A.P. Sherje, A. Surve and P. Shende, *J. Mater. Sci. Mater. Med.*, **30**, 74 (2019); https://doi.org/10.1007/s10856-019-6268-0
44. M.M. Maitre, M.R. Longhi and G.G. Granero, *Drug Dev. Ind. Pharm.*, **33**, 311 (2007); https://doi.org/10.1080/03639040600901978
45. T. Yamakawa and S. Nishimura, *J. Control. Release*, **86**, 101 (2003); https://doi.org/10.1016/S0168-3659(02)00367-X
46. S. Uppal, K. Kaur, R. Kumar, N.K. Kahlon, R. Singh and S.K. Mehta, *Ultrason. Sonochem.*, **39**, 25 (2017); https://doi.org/10.1016/j.ultsonch.2017.04.007
47. Y. Bai, C. Liu, F. Xie, R. Ma, L. Zhuo, N. Li and W. Tian, *Carbohydr. Polym.*, **213**, 411 (2019); https://doi.org/10.1016/j.carbpol.2019.03.017
48. Z. Wang and Y. Li, *Pharmaceutics*, **10**, 76 (2018); https://doi.org/10.3390/pharmaceutics10030076